arXiv:1608.02973v1 [cond-mat.soft] 9 Aug 2016

Chemically active colloids near osmotic-responsive walls with surface-chemistry gradients

M N Popescu, W E Uspal and S Dietrich

Max-Planck-Institut für Intelligente Systeme, Heisenbergstr. 3, 70569 Stuttgart, Germany

IV. Institut für Theoretische Physik, Universität Stuttgart, Pfaffenwaldring 57, 70569 Stuttgart, Germany

E-mail: popescu@is.mpg.de, uspal@is.mpg.de, dietrich@is.mpg.de

Abstract. Chemically active colloids move by creating gradients in the composition of the surrounding solution and by exploiting the differences in their interactions with the various molecular species in solution. If such particles move near boundaries, e.g., the walls of the container confining the suspension, gradients in the composition of the solution are also created along the wall. This give rise to chemi-osmosis (via the interactions of the wall with the molecular species forming the solution), which drives flows coupling back to the colloid and thus influences its motility. Employing an approximate "point-particle" analysis, we show analytically that – owing to this kind of induced active response (chemi-osmosis) of the wall – such chemically active colloids can align with, and follow, gradients in the surface chemistry of the wall. In this sense, these artificial "swimmers" exhibit a primitive form of thigmotaxis with the meaning of sensing the proximity of a (not necessarily discontinuous) physical change in the environment. We show that the alignment with the surface-chemistry gradient is generic for chemically active colloids as long as they exhibit motility in an unbounded fluid, i.e., this phenomenon does not depend on the exact details of the propulsion mechanism. The results are discussed in the context of simple models of chemical activity, corresponding to Janus particles with "source" chemical reactions on one half of the surface and either "inert" or "sink" reactions over the other half.

PACS numbers: 47.63.mf, 82.70Dd, 47.15.G,47.57.-s

Keywords: self-diffusiophoresis, chemi-osmosis, Stokes flow, chemically patterned walls

1. Introduction

Significant efforts have been made towards the development of small objects with sizes in the micrometer range and smaller, which are endowed with means of self-propulsion – and thus to be motile – in a liquid environment [1–18]. These artificial swimmers operate under non-equilibrium conditions such as the catalytic promotion of chemical reactions in the surrounding liquid. Their motion typically occurs within the regime of very small Reynolds (Re) numbers, and thus they represent potential benchmark

examples of inertia-less motility mechanisms [19–25]. Numerous theoretical [26–44] and numerical [45–51] studies have been devoted to various aspects of the motion of self-propelled colloids, ranging from motility mechanisms at the single-particle level ("active particles") [26–48] to the emergence of complex collective behaviors ("active fluids"), such as 'living" crystals [9,14,52,53], swarming [50,51,54,55], phase separations [51, 54, 56–58], or mesoscale active turbulence [49, 51].

One of the typical experimental realizations of self-propelled particles is that of colloids with a surface chemistry designed such as to promote catalytically activated chemical reactions in the surrounding liquid environment [1–7,10,11]). These chemically active colloids achieve motility through various mechanisms of converting "chemical" free energy, obtained from locally changing the chemical composition, into mechanical work. Among these mechanisms, one often encounters variants, such as diffusio- [7, 10, 14] or electrochemical- [1–4, 6] phoresis, which exploit the solvent mediated, effective interactions between the surface of the active particle and the reactant and product molecules [59, 60].

For chemically active colloids the motion originates from the coupling between the distribution of chemical species and the hydrodynamic flow fields produced by them [28,29,31,45]. Both of these fields are distorted by nearby interfaces, and therefore it is reasonable to expect non-trivial dynamics when active colloids move near confining surfaces. Recent reports indeed provide evidence for a very complex behavior. This includes the emergence of surface-bound steady-states [40, 61–63] and directed motion due to a spatially varying hydrodynamic slip boundary condition [64]. If the motion occurs near walls, and is in addition exposed to external flows or fields, other remarkable features such as rheotaxis of spherical colloids [65] and gravitaxis [15, 66, 67] appear.

These phenomena become even richer if the confining surface is by itself responsive (in addition to its "inert" role of reflecting the chemical and hydrodynamic flow fields) to, e.g., the chemical inhomogeneities induced by the activity of the colloid. One class of such examples is the case of a fluid-fluid interface, the surface tension of which depends on the distribution of various molecules across the interfacial region. It has been shown that in such cases the chemical activity of the particle can induce Marangoni stresses ‡, which for a colloid trapped at the interface lead to self-propulsion along the interface [41, 69], or to an effective, long-ranged interaction of the colloid with an interface located in its proximity [70].

Another class of such surfaces is that of walls on which, in analogy with phoresis, chemi-osmotic flows can be induced if the chemical composition of the solution varies along the wall [59, 60]. This results in chemi- (or thermo-) osmotic flows, which extend in the bulk, couple back to the colloid, and induce "drift" along the surface. Various studies have sought to characterize these flows. In order to induce osmotic flows, either variations in the composition of the solution have been employed, e.g., due to

‡ Since the surface tension is temperature dependent, a similar phenomenon arises if the particle is thermally active, e.g., by being heated partially with a laser, rather than chemically active (see, e.g., Refs. [43, 68]).

an active colloid in the vicinity of the surface (such as in the studies of "surfers" in Refs. [9, 52, 71, 72]), or temperature variations along the wall due to hot particles embedded in or glued to the surface [73].

The motility of self-phoretic active colloids near such surfaces amounts to a complex interplay between self-phoresis and the chemi-osmotic response of the surface, with the latter strongly depending on the material identity of the wall. For example, it has been shown recently that chemical steps and stripes of the wall can dock or spatially confine the motion of chemically active colloids [74]. This naturally leads to the expectation, which we shall explore here, that a chemically active colloid may detect and follow – through an induced chemi-osmotic response – gradual spatial gradients in the chemistry of a nearby wall. Such a behavior is a simple form of thigmotaxis, here with the meaning of sensing the proximity of a physical change (not necessarily discontinuous) in the environment.

In the following we focus on the particular case of a spherical colloid with an axisymmetric chemical activity caused by a corresponding catalyst distribution. The colloid is considered to be constrained to move with its axis parallel to the wall. The wall is responsive via chemi-osmotic flows, and the chemistry of the wall varies laterally. We employ a point-particle approximation which has been shown [70, 74] to capture the relevant phenomenology in almost quantitative agreement with the results obtained from exact numerical calculations. Within this approach we obtain simple, physically intuitive expressions for the translation- and rotation- contributions for the dynamics of the colloid induced by the chemi-osmotic response of the patterned wall. Based on these results we predict that in the case of motion near a wall with a constant, linear chemical gradient, the active particle will align with the direction of the gradient. These general results are then discussed in the context of simple models of active colloids defined by suitably selecting the "activity function" (see, c.f., Section 2 for a precise definition). This amounts to prescribing a specific chemical reaction at each point on the surface such as to mimic either a net production of a solute by the particle, or a particle which emits and annihilates the solute so that there is no net production.

The organization of the paper is as follows. In Section 2 we define the model, present the governing equations, and derive the contributions of the chemi-osmotic response of the patterned wall to the motion of the particle. Section 3 is devoted to an analysis and a discussion of the emergence of thigmotaxis of active particles exhibiting various model activity functions. A summary and the conclusions of the study are presented in Section 4.

2. Model system

The system of interest is that of a chemically active colloid of radius R (figure 1(a)), moving above a planar wall which has a spatially non-uniform surface chemistry, as depicted in figure 1(b). The colloid is suspended in a Newtonian, incompressible solution of viscosity μ. For simplicity, we consider the colloid to have a uniform mass density and

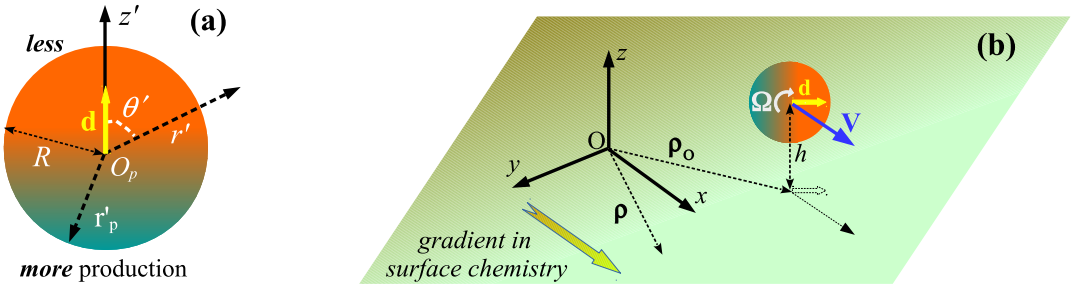

Figure 1. (a) Schematic drawing of a spherical, chemically active colloid with an activity function which is axisymmetric but lacks fore-aft symmetry. The orientation of the colloid is described by the unit vector **d** (yellow arrow), which points towards the north pole where less solute is produced. O_p denotes the center of the particle of radius R. (b) An active colloid, as in (a), moving laterally with $\mathbf{d} \perp \mathbf{e}_z$ at a height h (measured from the center of the colloid) above the planar wall (x, y) located at $z = 0$. The color of the plane indicates a linear gradient in the surface chemistry of the wall. Due to the chemi-osmotic flow response of the wall, the velocity **V** of the particle (blue arrow) is not necessarily aligned with **d** (which would be the case in an unbounded ("bulk") solution, panel (a)); this is illustrated by the thin arrows in the plane $z = 0$ below the particle showing the corresponding projection of **d** and **V**, respectively. The lateral position of the center of the particle is denoted as $\boldsymbol{\rho}_0$.

to be density-matched to the solution. The chemical activity of the colloid is modeled as the release into (or annihilation from) the solution of solute molecules A which are diffusing in the solution with diffusion constant D. The activity at various parts of the surface of the colloid can be different with respect to both the magnitude and/or the source/sink character. In figure 1(a) this is depicted by a variation in the color of the surface. Both the colloid and the wall are impermeable to solvent and solute. The molecules of species A interact with the surface of the colloid, as well as with the surface of the wall. In addition to the surfaces being impermeable, these interactions differ from the corresponding ones of the solvent molecules and are assumed to be very short ranged so that they are significant only within a distance $\delta \ll R$ from the surface. The interactions between the A molecules and those of the solvent are accounted for by the viscosity μ of the solution. The whole system is in contact with a solute reservoir which prescribes the bulk far from the colloid, i.e., the chemical potential and, implicitly, the number density c_∞ of species A. We further assume that the number density $\tilde{c}(\mathbf{r})$ of A molecules is everywhere sufficiently small so that they can be treated as an ideal gas.

For molecular species in water-like solvents and for colloids of μm in size moving with a velocity of the order of μm/s, the diffusional relaxation of the solute distribution over distances of the order of R is very small. Furthermore, the solution flows with velocities of the same order as that of the colloid; thus the Reynolds number $\mathrm{Re} := \rho_m V R/\mu$ (with ρ_m the mass density of the solution) and the Péclet number of the solute $\mathrm{Pe} := RV/D$ are both very small: $\mathrm{Re},\ \mathrm{Pe} \ll 1$. Therefore the hydrodynamics can be described by the Stokes equations, the advective transport of solute can be neglected

relative to that by diffusion, and the dynamics of $\tilde{c}(\mathbf{r})$ can be analyzed within a quasi-adiabatic approximation describing the steady-state distribution at the instantaneous position of the colloid.

2.1. Chemically active particle in an unbounded fluid

The motion of such chemically active model colloids in unbounded fluids has been studied in detail [26,28,30,34,36]. For completeness and convenience here we succinctly summarize the main results. As discussed before, we consider only the case of surface activities which are axisymmetric; this defines $\mathbf{d}$ (see figure 1(a)). For some of the calculations, it turns out to be convenient to use a system of coordinates (indicated by primed quantities) with the origin at the center O_p of the colloidal particle and the z'-axis oriented along the symmetry axis so that $\mathbf{e}_{z'} = \mathbf{d}$. With respect to this system, the spherical coordinates (r', θ', ϕ') are introduced in the usual way (see figure 1(a)).

The excess over the equilibrium, bulk number density of solute $c(\mathbf{r}') := \tilde{c}(\mathbf{r}') - c_\infty$ obeys the Laplace equation

$$\nabla'^2 c = 0\,, \tag{1}$$

subject to the boundary conditions

$$c(|\mathbf{r}'| \to \infty) = 0 \tag{2a}$$

and

$$[\mathbf{e}_{r'} \cdot (-D\nabla' c)]_{r'=R} = Q f(\theta')\,, \tag{2b}$$

where Q (with the units $\mathrm{m}^{-2}\mathrm{s}^{-1}$ of a number density current) is chosen with the sign convention $Q > 0$ (see below). Equation (2*b*) provides the meaning of the "chemical activity" for the class of models which we consider §. It consists of a current along the direction $\mathbf{e}_{r'}$, i.e., along the direction of the inner normal $\mathbf{n}$ of the surface of the particle, which points into the fluid. This current is released into the solution at points $\mathbf{r}'_p := (R, \theta', \phi')$ on the surface (for $\mathbf{r}'_p$ see figure 1(b)) if $f(\theta') > 0$, and removed from the solution if $f(\theta') < 0$. The points with $f(\theta') = 0$ are "chemically inert": at these points equation (2*b*) reduces to the condition of an impermeable wall. The dimensionless function $f(\mathbf{r}'_p)$, which completes the definition of a specific model, is referred to as the "activity function". It encodes all the details related to the kinetics and to the mechanisms of the chemical reactions.

Due to axial symmetry, the solution [28]

$$c(r', \theta') = C_0 \sum_{n \geq 0} a_n \left(\frac{R}{r'}\right)^{n+1} P_n(\cos\theta') \tag{3}$$

of equations (1), (2*a*), and (2*b*) is independent of ϕ'; $\mathbf{r}'$ denotes a position vector measured from the center O_p of the particle, P_n denotes the Legendre polynomial of

§ In general, it can be expected that the right hand side of equation (2*b*) takes a more involved form, accounting for the densities of various reactant and product species, their different diffusivities, etc.

degree n, $C_0 := (QR)/D$ is a characteristic number density, and the dimensionless coefficients a_n are given by

$$a_n = \frac{2n+1}{2(n+1)} \int_0^\pi \mathrm{d}\theta' \sin\theta' f(\theta') P_n(\cos\theta') \,. \tag{4}$$

Equation (3) amounts to a multipole expansion, where the first term describes the number density due to a monopole of strength $4\pi QR^2 a_0$ located at O_p, the second term the density due to a dipole of strength $4\pi QR^3 a_1$ located at O_p and oriented parallel to $\mathbf{d}$, etc. We recall that $c(\mathbf{r}')$ is defined relative to the equilibrium value c_∞ in the bulk, and thus it can be positive (excess) or negative (depletion). In this sense, each of the terms in the expansion (3) of $c(\mathbf{r}')$ (such as the "dipole" one characterized by the dependence on $\cos\theta'$) carries a specific physical meaning.

Provided that the interaction potential $\Phi(\mathbf{r})$ of the solute molecules (relative to that of the solvent molecules [34, 36, 60]) with the surface of the colloid is short ranged as a function of the distance from the surface, this interaction is encoded in a so-called phoretic mobility coefficient [60]

$$b(\mathbf{r}_p) := (\beta\mu)^{-1} \int_0^\infty \mathrm{d}\xi \, \xi \left[\mathrm{e}^{-\beta\Phi(\mathbf{r}_p + \xi\mathbf{n})} - 1 \right] \,, \tag{5}$$

where β denotes the inverse of the thermal energy $k_B T$. The dependence of b on $\mathbf{r}_p$ exhibits the same symmetries as the activity. For the type of active colloids we are focusing on, this means that $b(\mathbf{r}_p)$ at a point P on the surface with position vector $\mathbf{r}_p$, or $\mathbf{r}'_p$ in the primed system, depends only on θ' (see figure 1(a)). The effect of the coupling to the gradient of the solution composition on the dynamics of the colloid and of the solution is accounted for by a so-called phoretic slip hydrodynamic boundary condition at the surface of the colloid. According to the latter, the hydrodynamic flow $\mathbf{u}$ of the solution is prescribed to take a non-zero value at the surface of the colloid [26, 34, 36, 60]:

$$\mathbf{u}(\mathbf{r})|_{\mathbf{r}=\mathbf{r}_p} = \mathbf{u}_s(\mathbf{r}_p) := -b(\mathbf{r}_p) \nabla_{||} c(\mathbf{r}_p) \,, \tag{6}$$

where $\nabla_{||}$ denotes the projection of ∇ onto the tangent plane of the surface. The coefficient b can be either positive or negative, depending on whether the character of the interaction Φ is attractive or repulsive; for repulsive interactions one has $b < 0$.

The hydrodynamic flow is obtained by solving the incompressible Stokes equations subject to the boundary condition in (6) and to the one of a quiescent solution at infinity (for more details see, e.g., [75–77]). If the spherical, chemically active colloid moves in an unbounded ($b$ulk) fluid and in the absence of external forces or torques acting on it or on the fluid, one finds the following simple expression for the velocity [28, 60, 75]:

$$\mathbf{V}^{(b)} = -(4\pi R)^{-2} \int_{|\mathbf{r}|=R} \mathrm{d}S \, \mathbf{u}_s(\mathbf{r}_p) \,. \tag{7}$$

In this case the axial symmetry of the system allows only for translation of the colloid along the direction defined by $\mathbf{d}$ (see figure 1(a)). If b varies sufficiently weakly across

the surface so that b can be taken to be a constant, (7) reduces to the very simple form $\mathbf{V}^{(b)} = \frac{2}{3}\frac{bQ}{D}a_1\,\mathbf{d}$, which holds for any activity function and allows one to identify the velocity scale

$$V_0 := \frac{|b|Q}{D}\,. \tag{8}$$

For Janus colloids, which are half-covered by catalyst, one finds as typical experimental values $|\mathbf{V}^{(b)}| \simeq 5\ \mu$m/s [7,17,18,62]. The above simple model with uniform b, applied to the specific case of "constant flux" activity over half of the surface while the other half is chemically inert (for which $|a_1| = 3/8$, see, c.f., section 3.2), predicts $|\mathbf{V}^{(b)}| = V_0/4$ [28]. This leads to the estimate $V_0 \simeq 20\ \mu$m/s.

2.2. Motion of chemically active particles near responsive walls

We now consider the motion of chemically active colloids near a planar wall, located at $z = 0$ (see figure 1 (b)), which is "responsive" in a sense defined below. The solute number density $c(\mathbf{r})$ obeys the Laplace equation (1), subject to the boundary condition far from the particle (at infinity) given by $(2a)$, the boundary condition at the surface of the particle given by $(2b)$, and the additional boundary condition of impermeability at the wall

$$[\mathbf{e}_z \cdot (-D\nabla c)]_{z=0} = 0\,. \tag{9}$$

(The *interior* normal to the wall is $\mathbf{e}_z$, see figure 1 (b).) The solution of the boundary-value problem defined above provides the number density $c(\mathbf{r})$ of solute.

As discussed above, besides the impermeability condition the solute molecules interact both with the colloid and with the wall. These interactions are taken to be short ranged as functions of the distances from the corresponding surfaces. Denoting the interaction potential of a molecule A with the wall by $\Psi(\mathbf{r})$, the effect of this interaction and of the variations of the excess solute number density $c(\boldsymbol{\rho})$ along the wall (where $\boldsymbol{\rho}$ is the in-plane position vector, see figure 1 (b)) is, in analogy with the situation at the surface of the colloid, a chemi-osmotic shear stress along the wall [59, 60]. This is accounted for by a chemi-osmotic slip hydrodynamic boundary condition at the surface of the wall [59, 60]:

$$\mathbf{u}(\mathbf{r})|_{z=0} = \mathbf{u}_c(\boldsymbol{\rho}) := -b_w(\boldsymbol{\rho})\nabla_{||}c(\boldsymbol{\rho})\,, \tag{10}$$

with the chemi-osmotic mobility coefficient b_w given by

$$b_w(\boldsymbol{\rho}) := (\beta\mu)^{-1}\int_0^\infty \mathrm{d}\xi\,\xi\left[\mathrm{e}^{-\beta\Psi(\boldsymbol{\rho}+\xi\mathbf{e}_z)} - 1\right]\,. \tag{11}$$

The slip velocity $\mathbf{u}_c$ (where the subscript "c" refers to *c*hemi-osmosis) in (10) and (11) defines the meaning of a chemi-osmotic response of the wall: if the interaction of the solute with the wall reduces to the condition that the wall is impermeable, i.e., $\Psi \equiv 0$, one has $b_w \equiv 0$ and $\mathbf{u}_c \equiv 0$, which corresponds to the motion near an inert wall. This

reduces to a no-slip boundary condition at the wall, which solely reflects back the solute distribution and the hydrodynamic flow. This was studied in detail in [40, 65].

The hydrodynamic flow $\mathbf{u}(\mathbf{r})$ of the solution obeys the incompressible Stokes equations

$$\nabla \cdot \hat{\boldsymbol{\sigma}} = 0\,, \qquad \nabla \cdot \mathbf{u} = 0\,, \tag{12}$$

where $\hat{\boldsymbol{\sigma}} := -p\hat{\mathrm{I}} + \mu\,[\nabla\mathbf{u} + (\nabla\mathbf{u})^{\mathrm{t}}]$ denotes the stress tensor (of a Newtonian fluid), p is the pressure, $\hat{\mathrm{I}}$ is the identity tensor of rank three, and the superscript "t" denotes the transpose. (We also use the common convention that two adjacent vectors (or vector operators) without a dot or cross product sign between them denotes the tensorial (dyadic) product.) The Stokes equations are to be solved subject to the following boundary conditions (at the instantaneous position of the colloid):
- quiescent fluid far from the colloid,

$$\mathbf{u}(|\mathbf{r}| \to \infty) = 0\,, \tag{13a}$$

- phoretic slip (known from (6)) at the surface of the colloid (which has rigid body translational and rotational velocities $\mathbf{V}$ and $\boldsymbol{\Omega}$, respectively),

$$\mathbf{u}(\mathbf{r} = \mathbf{r_p}) = \mathbf{V} + \boldsymbol{\Omega} \times (\mathbf{r}_p - \mathbf{r}_{O_p}) + \mathbf{u}_s(\mathbf{r}_p)\,, \tag{13b}$$

where $\mathbf{r}_{O_p}$ denotes the position vector of the center of the colloid, and
- osmotic slip (known from (10)) at the wall,

$$\mathbf{u}(\mathbf{r} = \boldsymbol{\rho}) = \mathbf{u}_c(\boldsymbol{\rho})\,. \tag{13c}$$

The boundary value problem posed above is closed by the requirement of steady-state motion of the colloid without inertia, i.e., the forces and torques acting on the colloid are balanced:

$$\mathbf{F}_{hyd} + \mathbf{F}_{ext} = 0\,, \qquad \mathbf{T}_{hyd} + \mathbf{T}_{ext} = 0\,, \tag{14}$$

where the subscript "*hyd*" refers to the hydrodynamic force and torque (due to the flow $\mathbf{u}$), while "*ext*" refers to any externally imposed forces and torques (e.g., due to gravity).

Depending on the particular system under study here, either $\mathbf{F}_{ext}$ and $\mathbf{T}_{ext}$ are given, and the problem is solved for $\mathbf{V}$ and $\boldsymbol{\Omega}$, or the velocities $\mathbf{V}$ and $\boldsymbol{\Omega}$ are given and the force $\mathbf{F}_{ext}$ and the torque $\mathbf{T}_{ext}$ required to achieve that state of motion are calculated. (These are often called the "drag" and the "force" problem, respectively [77].) Mixed problems are also common, in which some of the components of the external forces and torques as well as some of the components of the velocities are prescribed, all the remaining components being the unknowns for which the problem should be solved. We consider here, similarly to the discussion in [74], the case that the particle motion is constrained to proceed in a plane at height h above the wall, with orientation $\mathbf{d} \perp \mathbf{e}_z$ but otherwise free to rotate in-plane. While it might be challenging to implement these restrictions experimentally (see the discussion in [74]), this configuration has the advantage of allowing a clear identification of the effects due to the response of the wall, as well as that of facilitating analytically tractable theoretical arguments which lead to

closed form, physically intuitive results. Thus the hydrodynamics problem to be solved is that of a sphere, with phoretic-slip boundary condition at its surface, translating with velocity $\mathbf{V} \perp \mathbf{e}_z$ and rotating with angular velocity $\mathbf{\Omega} = \Omega \mathbf{e}_z$ at a fixed height h above a wall with chemi-osmotic slip boundary condition. The particle is subject to an external force $\mathbf{F}_{ext} = F_{ext}\mathbf{e}_z$, which will be determined by requiring that it enforces the constraint $V_z = 0$, and to an external torque $\mathbf{T}_{ext} \perp \mathbf{e}_z$, the x and y components of which are determined by requiring that they enforce the constraints $\Omega_x = 0$ and $\Omega_y = 0$.

Taking advantage of the linearity of the Stokes equations and of the boundary conditions, the problem defined above is solved by superposing the solutions of the following two sub-problems (see [74]).

The `first sub-problem` (referred to by the label "sd") is that of *s*elf-*d*iffusiophoresis of a sphere, with phoretic slip boundary condition, $(13b)$, at its surface, and moving near a planar wall where the *no-slip* boundary condition holds. In the absence of thermal fluctuations (which in general are neglected in the present study), owing to the axial symmetry of the colloid the motion proceeds in the plane which is orthogonal to the wall and contains $\mathbf{d}$. We further require that the motion is constrained to satisfy $\mathbf{d} \perp \mathbf{e}_z$ and that the center of the particle remains located at a height h above the wall. Under these conditions, the *s*elf-*d*iffusiophoretic velocity of the particle is denoted by $\mathbf{V}^{(sd)}$ which, although not explicitly indicated, depends on h. These constraints are imposed by an external force $\mathbf{F}^{(sd)} = F^{(sd)}\mathbf{e}_z$ and an external torque $\mathbf{T}^{(sd)} = T_x^{(sd)}\mathbf{e}_x + T_y^{(sd)}\mathbf{e}_y$, which are determined by requiring $V_z^{(sd)} = 0$ and $\Omega_x^{(sd)} = \Omega_y^{(sd)} = 0$. Due to the symmetry of the system, this implies $\mathbf{V}^{(sd)} = V^{(sd)}\mathbf{d}$. This problem was studied in detail in [40, 62, 63]. Therefore, here we simply note that $\mathbf{V}^{(sd)}$ and the constraining quantities $\mathbf{F}^{(sd)}$ and $\mathbf{T}^{(sd)}$ can be calculated for a given height h and a given phoretic mobility coefficient $b(\mathbf{r}_p)$. In the following, we take $V^{(sd)}(h)$ as a parameter which is of the same order of magnitude as $V^{(b)}$.

The `second sub-problem` (referred to by the label "w" which stands for *w*all response) is that of a sphere, with no-slip boundary conditions at its surface, translating with velocity $\mathbf{V}^{(w)} \perp \mathbf{e}_z$, and rotating with angular velocity $\mathbf{\Omega}^{(w)} = \Omega_z^{(w)}\mathbf{e}_z$ at a constant height h above a wall at which a chemi-osmotic slip boundary condition, $(13c)$, holds. The constraints on the motion are imposed by an external force $\mathbf{F}^{(w)} = F^{(w)}\mathbf{e}_z$ and an external torque $\mathbf{T}^{(w)} = T_x^{(w)}\mathbf{e}_x + T_y^{(w)}\mathbf{e}_y$, which are determined by requiring $V_z^{(w)} = 0$ and $\Omega_x^{(w)} = \Omega_y^{(w)} = 0$. The solution of this second sub-problem, which provides the contribution of the induced response by the wall to the motion of the particle, is the focus of the remainder of the paper.

Before proceeding, we remark that from the solutions of the two sub-problems the translational and rotational velocities of the particle follow as $\mathbf{V} = \mathbf{V}^{(sd)} + \mathbf{V}^{(w)}$ and $\mathbf{\Omega} = \mathbf{\Omega}^{(w)}$ (because the self-diffusiophoresis sub-problem is constrained to not involve rotations), respectively. The force $\mathbf{F}_{ext}$ and the torque $\mathbf{T}_{ext}$, needed to ensure the desired in-plane motion, are given by the sums of the corresponding contributions ("sd" and "w") from the two sub-problems.

2.3. The contributions to the motion due to the induced response by the wall

The calculation of the induced response by the wall involves two steps. The first one consists of determining the distribution of the solute $c(\boldsymbol{\rho})$ at the wall, which is needed in order to find the chemi-osmotic slip $\mathbf{u}_c(\boldsymbol{\rho})$, (10), for the hydrodynamic boundary condition. The second step requires solving, having determined $\mathbf{u}_c(\boldsymbol{\rho})$ in the first step, the second hydrodynamics sub-problem formulated in the previous subsection.

Since we seek the qualitative phenomenology and physically intuitive results, rather than aiming at a quantitative study, for both steps we employ a point-particle (far-field) approximation and keep only few terms in the corresponding multipole expansions. (Nevertheless, we keep a sufficient number of terms in order to capture the relevant symmetries of the solute distribution at the wall, and thus of the wall-driven flows.) Such an approach has been employed successfully in previous studies (see, e.g., [22, 70] and, in particular, [74] which is closely related to the present study). In many cases it has turned out that this approximation captures very well, even semi-quantitatively, the phenomenology for particle center - wall distances as small as $h \gtrsim 1.5\,R$ [74].

Within the point-particle approximation, the (excess) density in the presence of the wall at $z = 0$ (with reflecting boundary condition, (9), corresponding to impermeability) can be constructed straightforwardly from the expansion in (3) by using the method of images: in the expansion (3), for each source term, located at the position $\mathbf{r}_{O_p} = \boldsymbol{\rho}_0 + \mathbf{z}_0$ of the center of the particle, an identical copy acting as an image term is placed at $\mathbf{r}^*_{O_p} = \boldsymbol{\rho}_0 - \mathbf{z}_0$. This ensures that the boundary condition (9) is satisfied by the sum $c(\mathbf{r}') + c_{image}(\mathbf{r}')$ of the source and image contributions. Here $\boldsymbol{\rho}_0 = x_0\mathbf{e}_x + y_0\mathbf{e}_y$ is the position vector of the projection of $\mathbf{r}_{O_p}$ onto the plane $z = 0$, $\mathbf{z} = z\mathbf{e}_z$, and $\mathbf{z}_0 = h\mathbf{e}_z$ (see figure 1). With $c(\mathbf{r}') = c(\mathbf{r} - \mathbf{r}_{O_p}) = c(\boldsymbol{\rho} - \boldsymbol{\rho}_0 + \mathbf{z} - \mathbf{z}_0)$ and $c_{image}(\mathbf{r}') = c(\boldsymbol{\rho} - \boldsymbol{\rho}_0 + \mathbf{z} + \mathbf{z}_0)$, due to $|\boldsymbol{\rho} - \boldsymbol{\rho}_0 - \mathbf{z}_0| = |\boldsymbol{\rho} - \boldsymbol{\rho}_0 + \mathbf{z}_0|$, it follows that the solution $c(\boldsymbol{\rho}, z = 0)$ fulfilling the boundary condition at the point $\boldsymbol{\rho} = x\mathbf{e}_x + y\mathbf{e}_y$, i.e., $z = 0$, is twice the expression in (3) evaluated at the wall, i.e., at $\mathbf{r}' = \boldsymbol{\rho} - \boldsymbol{\rho}_0 - \mathbf{z}_0$:

$$c(\boldsymbol{\rho}) = C_0 \sum_{n\geq 0} c^{(n)}(\boldsymbol{\rho})\,, \tag{15}$$

with the

- *m*onopole ($n = 0$) contribution

$$c^{(m)}(\boldsymbol{\rho}) := 2a_0 \frac{R}{|\boldsymbol{\rho} - \boldsymbol{\rho}_0 - \mathbf{z}_0|}\,, \tag{16a}$$

- *d*ipole ($n = 1$) contribution

$$c^{(d)}(\boldsymbol{\rho}) := 2a_1 \left(\frac{R}{|\boldsymbol{\rho} - \boldsymbol{\rho}_0 - \mathbf{z}_0|}\right)^2 \cos\theta'\,, \tag{16b}$$

- *q*uadrupole ($n = 2$) contribution

$$c^{(q)}(\boldsymbol{\rho}) := a_2 \left(\frac{R}{|\boldsymbol{\rho} - \boldsymbol{\rho}_0 - \mathbf{z}_0|}\right)^3 \left(3\cos^2\theta' - 1\right)\,, \tag{16c}$$

- *octopole* ($n = 3$) contribution

$$c^{(o)}(\boldsymbol{\rho}) := a_3 \left(\frac{R}{|\boldsymbol{\rho} - \boldsymbol{\rho}_0 - \mathbf{z}_0|} \right)^4 \left(5\cos^2\theta' - 3 \right) \cos\theta' \,, \;\; etc. \tag{16d}$$

The angle θ' between $\mathbf{d}$ and $\mathbf{r}'$ is given by

$$\cos\theta' = \frac{\mathbf{d}\cdot\mathbf{r}'}{|\mathbf{r}'|} \overset{(\mathbf{d}\perp\mathbf{e}_z)}{=} \mathbf{d}\cdot\frac{\boldsymbol{\rho}-\boldsymbol{\rho}_0}{|\boldsymbol{\rho}-\boldsymbol{\rho}_0-\mathbf{z}_0|} \,. \tag{17}$$

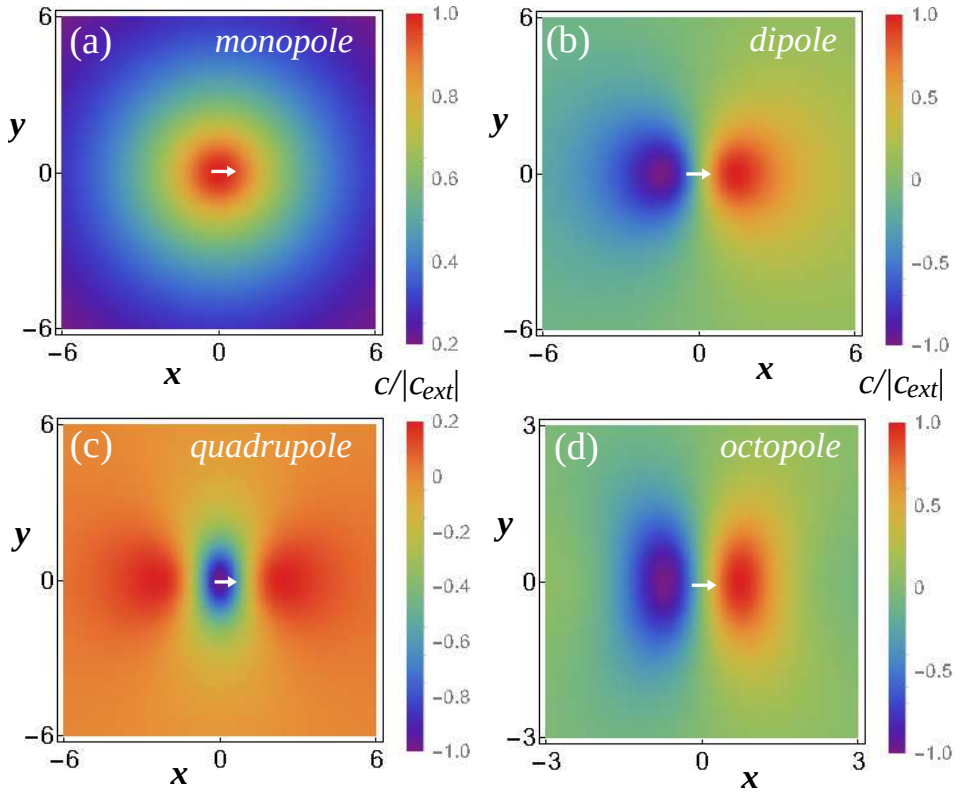

Figure 2. Various density distributions $c(\boldsymbol{\rho} - \boldsymbol{\rho}_0)$ at the wall $z = 0$ (color coded) in units of the absolute values $|c_{ext}|$ of their corresponding extrema. The panels show the monopole, dipole, quadrupole, and octopole contributions (see (16a) - (16d)) of an active particle located at $h = 2R$ above the lateral position $\boldsymbol{\rho}_0$. All distances are measured in units of the particle radius R. The white arrows indicate the projections $\mathbf{d}_{||}$ of $\mathbf{d}$ onto the plane $z = 0$. The considered ranges of values (see the color bar to the right of each plot) differ between the four panels. For reasons of clarity panel (d) shows only a smaller region around the lateral position $\boldsymbol{\rho}_0$ of the center O_p of the particle.

In figure 2 we illustrate each multipole contribution, (16a) - (16d), to the excess number density at the wall for the particular value $h = 2\,R$. It can be seen that, as borne out by (16a), the monopole contribution is the *only* one with in-plane radial symmetry around the projection of the particle center P_O onto the plane $z = 0$. All the higher order ones exhibit in-plane mirror symmetry with respect to the line $\mathbf{d}_{||}$ (white arrows in figure 2) which is parallel to $\mathbf{d}$. Intuitively, one thus infers that if the chemical properties of the wall are anisotropic and exhibit a specific direction $\mathbf{d}'$ (as in, e.g., figure 1 (b)), which happens to be distinct from $\mathbf{d}$, the various terms in the expansion may cause

qualitatively different effects. The monopole contribution perceives "passively" the direction $\mathbf{d}'$ because this distribution, and therefore the response induced at the wall, is independent of the specific orientation of $\mathbf{d}_{||}$, i.e., of how the particle is oriented with respect to the anisotropy in the properties of the wall. The magnitude of $\nabla_{||}c^{(m)}$ depends only on the distance $|\boldsymbol{\rho}-\boldsymbol{\rho}_0|$ from the lateral position $\boldsymbol{\rho}_0$. However, since b_w varies along $\mathbf{d}'$ the magnitude of the chemi-osmotic slip depends on the position $\boldsymbol{\rho}-\boldsymbol{\rho}_0$, and not only on this distance. Therefore, along the direction $\mathbf{d}'$ the response of the wall, in the form of chemi-osmotic flows, does not have fore-aft symmetry. Hence it induces a translation of the colloid along $\mathbf{d}'$. This translation is independent of the orientation of $\mathbf{d}_{||}$ relative to that of $\mathbf{d}'$. However, the higher order terms offer the means for competing effects and the interplay between the "wall preferred" symmetry characterized by $\mathbf{d}'$ and the "density preferred" one $\mathbf{d}_{||}$. Since the particle is allowed to undergo in-plane rotations, $\mathbf{d}$ is actually free to rotate. This can lead to the selection of certain orientations of $\mathbf{d}$ with respect to $\mathbf{d}'$ so that an "active" sensing of $\mathbf{d}'$ emerges. This point will be analyzed in detail in, c.f., section 3. We also remark that with respect to the line $\mathbf{d}_\perp$ in the plane of the wall, which passes through the projection P_O and is perpendicular to $\mathbf{d}_{||}$, the even-n multipole contributions are mirror-symmetric (fore-aft symmetry), while the odd-n ones are mirror-antisymmetric (i.e., corresponding to reflection and a change in sign), and thus their fore-aft symmetry is broken. The latter implies that there is, e.g., a response which has also a directionality with respect to $\mathbf{d}_{||}$ (i.e., it can give rise to *surfing* [72]). Finally, as can be easily inferred from (16a) - (16d), the magnitude of the contributions decreases steeply with increasing order n, and thus the first few terms dominate the behavior of the density $c(\boldsymbol{\rho})$, (15), for in-plane distances $|\boldsymbol{\rho}-\boldsymbol{\rho}_0|/R \gtrsim 3$.

We now proceed to the solution of the second hydrodynamic sub-problem. Since here only the translational velocity $\mathbf{V}^{(w)}$ and the angular velocity $\boldsymbol{\Omega}^{(w)}$ of the particle are of particular interest, we approach this hydrodynamic sub-problem by using the Lorentz reciprocal theorem [77–80]. This states that, in the absence of volume forces, any two solutions $\mathbf{u}_0(\mathbf{r})$ and $\mathbf{u}_a(\mathbf{r})$ of the incompressible Stokes equations within the same domain $\mathcal{D}$, i.e., solutions subject to different boundary conditions but on the very same boundaries $\partial\mathcal{D}$, obey the relation

$$\int\limits_{\partial\mathcal{D}} \mathbf{u}_0 \cdot \hat{\boldsymbol{\sigma}}_a \cdot \mathbf{n}\,\mathrm{d}S = \int\limits_{\partial\mathcal{D}} \mathbf{u}_a \cdot \hat{\boldsymbol{\sigma}}_0 \cdot \mathbf{n}\,\mathrm{d}S\,, \tag{18}$$

where $\hat{\boldsymbol{\sigma}}_0$ and $\hat{\boldsymbol{\sigma}}_a$ denote the stress tensors corresponding to the two flow fields. We choose for the problem "0" the above second sub-problem. For the so-called *a*uxiliary problem "a", we consider a sphere with radius R and no slip at its surface which is driven by certain forces $\mathbf{F}_a$ and torques $\mathbf{T}_a$. It moves with constant translational velocity $\mathbf{V}_a$ and angular velocity $\boldsymbol{\Omega}_a$ through a fluid at the same height h from a planar wall with *no slip* boundary condition:

$$\mathbf{u}_a|_{z=0} = 0\,. \tag{19}$$

The fluid is assumed to be quiescent far away from the particle, i.e., $\mathbf{u}_a(|\mathbf{r}| \to \infty) = 0$.

For our system the boundary $\partial\mathcal{D}$ consists of the surface of the sphere, the wall, and the surface S_∞ at infinity, e.g., a hemisphere (in the half plane $z > 0$) with a radius $R_\infty \to \infty$. Since both $\mathbf{u}_0(\mathbf{r})$ and $\mathbf{u}_a(\mathbf{r})$ decay at least $\propto |\mathbf{r}|^{-1}$ for $|\mathbf{r}| \to \infty$, the contributions from the integrals over S_∞ are vanishingly small. Thus only the integrals over the surface of the sphere and over the wall contribute to (18). By replacing the flows at the surfaces by the expressions for the corresponding boundary conditions (in the auxiliary problem, the boundary condition at the sphere has the same form as (13*b*) but with $\mathbf{V}_a$ and $\mathbf{\Omega}_a$ replacing the corresponding quantities and with $\mathbf{u}_s = 0$), by using that $\mathbf{V}^{(w)}$, $\mathbf{\Omega}^{(w)}$, $\mathbf{V}_a$, and $\mathbf{\Omega}_a$ are constant vectors (which allows one to factor them out of the integrals), and by noting that in each problem the hydrodynamic forces and torques must be exactly balanced by the forces and torques driving the colloid, one arrives at (for $\mathbf{u}_c$ see (10))

$$\mathbf{V}^{(w)} \cdot \mathbf{F}_a + \mathbf{\Omega}^{(w)} \cdot \mathbf{T}_a - \mathbf{V}_a \cdot \mathbf{F}^{(w)} - \mathbf{\Omega}_a \cdot \mathbf{T}^{(w)} = \int\limits_{z=0} \mathrm{d}S\, \mathbf{u}_c(\boldsymbol{\rho}) \cdot \hat{\boldsymbol{\sigma}}_a \cdot \mathbf{e}_z \,. \tag{20}$$

Since, by construction of the second sub-problem, $\mathbf{F}^{(w)}$ has only a z-component, while $\mathbf{T}^{(w)}$ has no z-component, for auxiliary problems which involve only translations along the x- or y-axis and/or rotations around the z-axis it follows that the last two terms on the left hand side of (20) vanish. In such cases, we obtain equations involving only the desired unknowns, i.e., $\mathbf{V}^{(w)}$ and $\mathbf{\Omega}^{(w)}$. Accordingly, we select the following three auxiliary problems, indexed by $a = 1, 2, 3$:

- $a = 1$: sphere translating along the x-axis (at $z = h$) due to a force $\mathbf{F} = F\mathbf{e}_x$;
- $a = 2$: sphere translating along the y-axis (at $z = h$) due to a force $\mathbf{F} = F\mathbf{e}_y$;
- $a = 3$: sphere spinning around the z-axis (at $z = h$) due to a torque $\boldsymbol{\tau} = \tau\mathbf{e}_z$.

In the first two auxiliary problems, due to the viscous friction on the sphere being larger on the side closer to wall, a rotation (rolling) occurs. Thus also a torque must be applied to the particle in order to achieve a purely translational motion. However, it turns out that this translation-rotation coupling is negligibly small unless the motion takes place very close to the wall, i.e., for $h/R \lesssim 1.1$ [81] (see also [40,74]), which is outside the range we are interested in. Therefore, in the first two auxiliary problems one can neglect these torques, which leads to a decoupling of the three equations (i.e., (20) with $a = 1, 2, 3$) and to the simple result

$$V_x^{(w)} = \int\limits_{z=0} \mathrm{d}S\, \mathbf{u}_c(\boldsymbol{\rho}) \cdot \frac{\hat{\boldsymbol{\sigma}}_1}{F} \cdot \mathbf{e}_z \,, \tag{21a}$$

$$V_y^{(w)} = \int\limits_{z=0} \mathrm{d}S\, \mathbf{u}_c(\boldsymbol{\rho}) \cdot \frac{\hat{\boldsymbol{\sigma}}_2}{F} \cdot \mathbf{e}_z \,, \tag{21b}$$

$$\Omega^{(w)} = \int\limits_{z=0} \mathrm{d}S\, \mathbf{u}_c(\boldsymbol{\rho}) \cdot \frac{\hat{\boldsymbol{\sigma}}_3}{\tau} \cdot \mathbf{e}_z \tag{21c}$$

with $\mathbf{u}_c$ given by (10).

For the stress tensors $\hat{\boldsymbol{\sigma}}_a$ corresponding to the auxiliary problems we use a point particle approximation. This is similar to the approach we have taken for calculating the density of solute at the wall. Under this approximation, the auxiliary problems reduce to those of the flows induced by point forces or torques located at $\mathbf{r}_{O_p}$, which have been calculated previously [75]. Due to the structure of (21a) - (21c), according to which $\mathbf{u}_c(\boldsymbol{\rho})$ has only the in-plane x- and y- components, only the components $\hat{\boldsymbol{\sigma}}_{a,xz}$ and $\hat{\boldsymbol{\sigma}}_{a,yz}$ are needed. At the wall, the so-called "tractions" $\mathbf{g} := \hat{\boldsymbol{\sigma}} \cdot \mathbf{e}_z$ are given by [74]

- $a = 1$ (point force $\mathbf{F} = F\mathbf{e}_x$):

$$\mathbf{g}_1 := \frac{\hat{\boldsymbol{\sigma}}_1}{F} \cdot \mathbf{e}_z = -\frac{3h}{2\pi}(x - x_0)\frac{\boldsymbol{\rho} - \boldsymbol{\rho}_0}{|\boldsymbol{\rho} - \boldsymbol{\rho}_0 - \mathbf{z}_0|^5}\,, \tag{22a}$$

- $a = 2$ (point force $\mathbf{F} = F\mathbf{e}_y$):

$$\mathbf{g}_2 := \frac{\hat{\boldsymbol{\sigma}}_2}{F} \cdot \mathbf{e}_z = -\frac{3h}{2\pi}(y - y_0)\frac{\boldsymbol{\rho} - \boldsymbol{\rho}_0}{|\boldsymbol{\rho} - \boldsymbol{\rho}_0 - \mathbf{z}_0|^5}\,, \tag{22b}$$

- $a = 3$ (point torque $\boldsymbol{\tau} = \tau\mathbf{e}_z$):

$$\mathbf{g}_3 := \frac{\hat{\boldsymbol{\sigma}}_3}{\tau} \cdot \mathbf{e}_z = -\frac{3h}{4\pi}\frac{(y - y_0)\mathbf{e}_x - (x - x_0)\mathbf{e}_y}{|\boldsymbol{\rho} - \boldsymbol{\rho}_0 - \mathbf{z}_0|^5}\,. \tag{22c}$$

The set of equations (20), (21a) - (21c), (15), (16a) - (16c), and (10) completes the calculation of the response induced by the wall. It provides $\mathbf{V}^{(w)}$ and $\boldsymbol{\Omega}^{(w)}$ in terms of a series of contributions arising from the corresponding multipole terms in the expansion of the density at the wall. In the following we restrict the discussion to the calculation of the angular velocity because it determines the emergence of thigmotaxis, the phenomenon which is the focus of the present study.

3. Results and discussion

The dependence of the chemi-osmotic mobility coefficient $b_w(\boldsymbol{\rho})$, (11), at the lateral position $\boldsymbol{\rho}$ on the wall reflects the chemical patterns occurring at the wall. The coefficient $b_w(\boldsymbol{\rho})$ must be a bounded function. However, in the following we shall consider also a linear dependence on $|\boldsymbol{\rho}|$; this should be interpreted physically as the case of a plate with a lateral extent being much larger than R or h, yet finite. This case is appealing due to its conceptual simplicity (similar to studies of rheotaxis which are employing a planar shear flow). It captures, as shown below, the alignment of the particle axis with the direction of the surface gradient. This allows one to follow the emergence of thigmotaxis without carrying out cumbersome algebra.

Before proceeding with specific choices for the spatial variations of the chemistry of the wall and for the activity function $f(\mathbf{r}'_P)$, we note that the steep decay of the tractions $\mathbf{g}_k,\ k = 1, 2, 3$, as functions of $|\boldsymbol{\rho} - \boldsymbol{\rho}_0|$ allows one to re-write the integrals in (21a) - (21c) in a more convenient form:

$$I_k := -\int\limits_{z=0} \mathrm{d}S\, b_w(\boldsymbol{\rho})\nabla_{||}c(\boldsymbol{\rho}) \cdot \mathbf{g}_k$$

$$= -\int\limits_{z=0} \mathrm{d}S\, \nabla_{||} \cdot [b_w(\boldsymbol{\rho}) c(\boldsymbol{\rho}) \mathbf{g}_k] + \int\limits_{z=0} \mathrm{d}S\, c(\boldsymbol{\rho}) \nabla_{||} \cdot [b_w(\boldsymbol{\rho}) \mathbf{g}_k]$$

$$= -\lim_{\rho_\infty \to \infty} \oint\limits_{\mathcal{C}_\infty} \mathrm{d}\phi\, \rho_\infty b_w(\boldsymbol{\rho}) c(\boldsymbol{\rho}) (\mathbf{g}_k \cdot \mathbf{e}_\rho) + \int\limits_{z=0} \mathrm{d}S\, c(\boldsymbol{\rho}) \nabla_{||} \cdot [b_w(\boldsymbol{\rho}) \mathbf{g}_k] \;,$$

where ρ_∞ denotes the radius of the contour $\mathcal{C}_\infty$ in the plane $z = 0$. Since $g_k(\rho \to \infty) \sim \rho^{-3}$ and $c(\rho \to \infty) \sim \rho^{-1}$, while at most $b_w(\rho \to \infty) \sim \rho$, the contour integral diminishes at least $\propto \rho_\infty^{-2}$ and therefore vanishes in the limit $\rho_\infty \to \infty$. Therefore

$$I_k = \int\limits_{z=0} \mathrm{d}S\, c(\boldsymbol{\rho}) \left[(\nabla_{||} b_w(\boldsymbol{\rho})) \cdot \mathbf{g}_k + b_w(\boldsymbol{\rho}) (\nabla_{||} \cdot \mathbf{g}_k) \right] . \tag{23}$$

This form provides particular insight into the calculation of the angular velocity $\Omega = I_3$, (21*c*) and (23), which determines the rotation of the particle axis $\mathbf{d}$. (We recall that, as discussed at the end of section 2.2, self-diffusiophoresis does not contribute to the in-plane rotations of the particle, i.e., $\Omega = \Omega^{(w)}$.) Since $\nabla_{||} \cdot \mathbf{g}_3 \equiv 0$ (which follows from (22*c*) by direct calculation), one arrives at

$$\Omega = \int\limits_{z=0} \mathrm{d}S\, c(\boldsymbol{\rho})\, \mathbf{g}_3 \cdot \nabla_{||} b_w(\boldsymbol{\rho}) \,. \tag{24}$$

From (24) it immediately follows that in the case of a spatially homogeneous chemistry of the wall (i.e., $b_w(\boldsymbol{\rho}) = const$) the angular velocity Ω vanishes identically (as it should, see the corresponding discussion in section 2.2). Thus in this case the induced response of the wall, i.e., the chemi-osmotic driven flow, cannot give rise to rotations of the axis of the active colloid.

3.1. Rotation in response to a constant surface-chemistry gradient

We now turn to the focus of the present study, which is a spatially constant gradient of the surface chemistry, as indicated in figure 1(b). We choose the coordinate system such that the x-axis coincides with the direction of the gradient. The orientation $\mathbf{d}_{||}$ of the particle can be expressed in terms of the corresponding orthogonal unit vectors:

$$\mathbf{d}_{||} = \cos\psi\, \mathbf{e}_x + \sin\psi\, \mathbf{e}_y \,. \tag{25}$$

Within this model, the chemi-osmotic mobility coefficient $b_w(\boldsymbol{\rho})$ takes the form

$$b_w(\boldsymbol{\rho}) \equiv b_w(x, y) = b_0 + \Delta\, x \,, \qquad \Delta > 0 \,, \tag{26}$$

which implies $b_w(0) = b_0$. In this case one has $\nabla_{||} b_w(\boldsymbol{\rho}) = \Delta\, \mathbf{e}_x$. From (24) and (22*c*) it follows that

$$\Omega = -\frac{3h\Delta}{4\pi} \int\limits_{-\infty}^{\infty} \mathrm{d}x \int\limits_{-\infty}^{\infty} \mathrm{d}y\, c(\boldsymbol{\rho})\, \frac{(y - y_0)}{|\boldsymbol{\rho} - \boldsymbol{\rho}_0 - \mathbf{z}_0|^5} \,. \tag{27}$$

The ratio in the last term of the integrand is an odd function of $y - y_0$, and each term in the expansion (15) of $c(\boldsymbol{\rho})$ has parity with respect to $y - y_0$ (see, e.g., (16*b*)

- (16c)). Therefore, only the terms in the expansion (15) which are odd functions of $y - y_0$ contribute to Ω; these terms correspond to odd values of the index n in (15).

Considering the first four terms ((16b) - (16c)) in the expansion of the density at the wall (see section 2.3), the above arguments imply that the monopole and quadrupole terms do not give rise to a rotation of the axis of the colloid. The angular velocity contribution due to the *d*ipole term is given by

$$\begin{aligned}\Omega^{(d)} &:= -\frac{3h\Delta}{4\pi}\int\limits_{z=0} \mathrm{d}S\, c^{(d)}(\boldsymbol{\rho})\,\frac{(y-y_0)}{|\boldsymbol{\rho}-\boldsymbol{\rho}_0-\mathbf{z}_0|^5}\\ &= -\frac{3a_1C_0R^2h\Delta}{2\pi}\int\limits_{z=0} \mathrm{d}S\,\frac{(x-x_0)(y-y_0)\cos\psi+(y-y_0)^2\sin\psi}{|\boldsymbol{\rho}-\boldsymbol{\rho}_0-\mathbf{z}_0|^8}\\ &= -\frac{3a_1C_0R^2h\Delta\sin\psi}{4\pi}\int\limits_{z=0} \mathrm{d}S\,\frac{|\boldsymbol{\rho}-\boldsymbol{\rho}_0|^2}{|\boldsymbol{\rho}-\boldsymbol{\rho}_0-\mathbf{z}_0|^8}\,,\end{aligned}$$

where in passing from the first line to the second we have used (16b) and (17), and in passing from the second to the third line we have used the fact that the first product in the nominator has odd parity with respect to both $(x - x_0)$ and $(y - y_0)$ and thus gives a vanishing contribution upon integration, while the integral of the second term is invariant with respect to the replacement $(y - y_0) \to (x - x_0)$. This leads to

$$\frac{\Omega^{(d)}}{\Omega_0} = -\frac{1}{8}a_1\left(\frac{R}{h}\right)^3\sin\psi\,, \tag{28}$$

with the characteristic angular velocity

$$\Omega_0 := \frac{C_0\Delta}{R} = \frac{Q\Delta}{D} > 0\,. \tag{29}$$

The contribution to the angular velocity due to the *o*ctopole term is given by

$$\Omega^{(o)} := -\frac{3h\Delta}{4\pi}\int\limits_{z=0} \mathrm{d}S\, c^{(o)}(\boldsymbol{\rho})\,\frac{(y-y_0)}{|\boldsymbol{\rho}-\boldsymbol{\rho}_0-\mathbf{z}_0|^5}\,. \tag{30}$$

The calculation of the integral is lengthy, but it involves steps similar to those leading to (28). Therefore we provide only the final result:

$$\frac{\Omega^{(o)}}{\Omega_0} = \frac{3}{64}a_3\left(\frac{R}{h}\right)^5\sin\psi\,. \tag{31}$$

Adding these contributions, one arrives at the following expression for the angular velocity due to the induced response at the wall:

$$\frac{\Omega}{\Omega_0} = \frac{1}{8}\left(\frac{R}{h}\right)^3\left[-a_1+\frac{3}{8}a_3\left(\frac{R}{h}\right)^2+\mathcal{O}\left(\left(\frac{R}{h}\right)^4\right)\right]\sin\psi\,. \tag{32}$$

The in-plane rotation of the axis $\mathbf{d}$ of the colloid due to the above contributions thus obeys the relation (see also (32))

$$\begin{aligned}&\frac{d\psi}{dt} = \Omega \quad \Rightarrow \quad \frac{d\psi}{dt} = A\Omega_0\sin\psi\\ &\Rightarrow \psi(t) = 2\arctan\left[e^{A\Omega_0 t}\tan\left(\frac{\psi(0)}{2}\right)\right]\end{aligned} \tag{33}$$

with

$$A := \frac{1}{8}\left(\frac{R}{h}\right)^3\left[-a_1 + \frac{3}{8}a_3\left(\frac{R}{h}\right)^2\right] . \tag{34}$$

This result has the following implications:
(i) The rotation of the axis depends only on the slope of the gradient of the osmotic mobility b_w, but not on any particular value of b_w such as $b_w(\boldsymbol{\rho}_0)$. Therefore the dynamics of the orientation of $\mathbf{d}$ with respect to the direction of $\nabla_{||}b_w$ does not depend on the initial position $\boldsymbol{\rho}_0$ of the center of the particle.
(ii) The angular velocity Ω vanishes at $\psi = \psi_\infty = 0, \pi$. Therefore the rotation of the axis (starting from a typical orientation $\psi(0) \neq 0, \pi$) is such that the asymptotic ($t \to \infty$) orientation of $\mathbf{d}$ is aligned with the direction of $\nabla_{||}b_w$, i.e., thigmotaxis emerges. For $A < 0$, the asymptotic value is $\psi_\infty = 0$, while for $A > 0$ it is $\psi_\infty = \pi$; therefore $\mathbf{d} \to \mathbf{e}_x$ and $\mathbf{d} \to -\mathbf{e}_x$, respectively.
(iii) In *leading* order in R/h, the angular velocity Ω carries a_1 as a prefactor (see (32)) which is the contribution of the dipole term in the expansion of the density ((3)). For an active colloid with a phoretic mobility $b(\mathbf{r}_P)$ which is approximately constant over the whole surface, this coefficient a_1 determines its velocity and thus its motile character in an unbounded fluid (see the corresponding expression for $\mathbf{V}^{(b)}$ above (8)). Therefore, if an active particle with such b exhibits motility when suspended in an unbounded fluid, i.e., $|\mathbf{V}^{(b)}| \neq 0$ and thus $a_1 \neq 0$, it will also exhibit thigmotaxis, i.e., $\Omega \neq 0$ for $\psi \neq 0, \pi$, if it is near a responsive wall with chemical gradients. In this sense, the emergence of thigmotaxis is a generic feature of chemically active colloids which are motile in an unbounded fluid. In other words, it is sufficient to know that in an unbounded fluid the colloid is motile – without knowing any other details about the mechanism (such as activity function) underlying the motion – in order to be able to predict that the same colloid will exhibit thigmotaxis when it is near a responsive wall with surface-chemistry gradients.
(iv) Under the same assumptions as in **(iii)**, to leading order in h/R the ratio of the angular velocity Ω and the translational velocity $V^{(b)}$ in an unbounded fluid is given by (for $a_1 \neq 0$)

$$\frac{\Omega}{V^{(b)}} = -\frac{3}{16}\frac{\Delta}{b}\left(\frac{R}{h}\right)^3 . \tag{35}$$

This ratio depends only on unexpectedly few material parameters and on the height to radius ratio. Most importantly, it is independent of any details of the activity function.

3.2. Dependence of the alignment with the wall pattern on the details of the chemical activity of the particle

Here, the general results obtained in the previous section will be discussed for three choices of the activity function $f(\theta)$ (see (2*b*)). These choices are typically employed in

studies of chemically active colloids [28]:

$$f^{(up)} = \begin{cases} 0, & 0 \leq \theta < \frac{\pi}{2} \\ +1, & \frac{\pi}{2} \leq \theta \leq \pi \end{cases}, \tag{36a}$$

$$f^{(vp)} = \begin{cases} 0 & 0 \leq \theta < \frac{\pi}{2} \\ -\cos\theta' & \frac{\pi}{2} \leq \theta \leq \pi \end{cases}, \tag{36b}$$

$$f^{(pa)} = \begin{cases} -1 & 0 \leq \theta < \frac{\pi}{2} \\ +1 & \frac{\pi}{2} \leq \theta \leq \pi \end{cases}. \tag{36c}$$

The first two choices with superscript (up) and (vp), respectively, describe a particle with *u*niform *p*roduction ((up)) or with a *v*ariable *p*roduction ((vp)) of a solute over the lower hemisphere (see figure 1(a)) while the upper hemisphere is chemically inactive (thus the particle is indeed a net producer of solute). The third choice with superscript (pa) describes a particle which *p*roduces a solute with a uniform rate Q over the lower hemisphere and *a*nnihilates it, at the same rate Q, over the upper hemisphere. Thus the particle is not a net producer of solute ‖. We note that in order for the model corresponding to the third choice to be well-defined, i.e., the density ((3)) to be positive everywhere, the bulk density c_∞ should be sufficiently large. For these activity functions, the first four coefficients $a_n, n = 0, \ldots, 3$ take the following values:

$$a_0^{(up)} = \frac{1}{2}, \quad a_1^{(up)} = -\frac{3}{8}, \quad a_2^{(up)} = 0, \quad a_3^{(up)} = \frac{7}{64}; \tag{37a}$$

$$a_0^{(vp)} = \frac{1}{4}, \quad a_1^{(vp)} = -\frac{1}{4}, \quad a_2^{(vp)} = \frac{5}{48}, \quad a_3^{(vp)} = 0; \tag{37b}$$

and

$$a_0^{(pa)} = 0, \quad a_1^{(pa)} = -\frac{3}{4}, \quad a_2^{(pa)} = 0, \quad a_3^{(pa)} = \frac{7}{32}. \tag{37c}$$

We remark that for the first and the third choice all coefficients with an even index $n > 0$ are zero, while for the second choice all coefficients with an odd index $n > 1$ are zero. The third choice has no monopole contribution, which is present in the first two choices. The second choice includes a quadrupole contribution ($a_2^{(vp)} \neq 0$), which is missing in the other two cases.

‖ All three choices are simple models of experimental realizations of active colloids. The first two correspond to the case of, e.g., a platinum (Pt)/silica Janus colloid decomposing peroxide (H_2O_2), with presumably only the Pt side being involved in the reaction. The third choice corresponds to the situation of a bi-metallic Janus colloid, e.g., Pt/gold(Au), decomposing H_2O_2 via oxidation/reduction mechanisms, for which both parts of the colloid surface contribute. (Pt is the production side, Au the annihilation side.) The reaction rate may be taken as spatially uniform (first and third choice) or as dependent on the spatial position due to, e.g., a dependence on the thickness of the catalyst layer [33, 82] (second choice). In all three cases the Damköhler number is considered to be small, i.e., the diffusion-reaction behavior of the H_2O_2 belongs to the reaction-limited regime.

For these three cases, up to the first two orders in R/h the factor A, (34), is given by

$$A^{(up)} = \frac{3}{64}\left(\frac{R}{h}\right)^3\left[1-\frac{7}{64}\left(\frac{R}{h}\right)^2\right] > 0\,, \qquad A^{(pa)} = 2A^{(up)} > 0\,,$$

and ((34) and (37b))

$$A^{(vp)} = \frac{1}{32}\left(\frac{R}{h}\right)^3 > 0\,. \tag{38}$$

Therefore, in each of the three cases the response from the wall aligns the colloid such that $\mathbf{d} = -\mathbf{e}_x$, i.e., against the direction of the gradient. This corresponds to a configuration of the colloid such that its solute producing side faces larger values of b_w. This behavior is expected intuitively and is consistent with the findings of the study in [74]. From this analysis we conclude that the thigmotaxis phenomenology depends only weakly (via quantitative differences between the corresponding angular velocities) on the precise details of the chemical activity and thus the motility mechanism.

The relevance of the rotation towards the surface-chemistry gradient, characterized by Ω, can be estimated by comparing it with the rotational diffusion of the colloid, characterized by the rotational diffusion coefficient D_R. To this end, for reasons of simplicity we discuss only the case (vp). Furthermore, for the purpose of a qualitative comparison we use the expression $D_R = (3/4)D_T R^{-2}$ [7] (where D_T denotes the translational diffusion coefficient of the particle) for the rotational diffusion coefficient of the spherical particle in an unbounded fluid. For a Janus particle with $R = 1$ μm and with a uniform phoretic mobility b, which in an unbounded fluid moves with velocity $V^{(b)} \sim 5$ μm/s (see section 2.1 and the discussion after (8)), the translational diffusion coefficient of the particle in water at room temperature (with viscosity $\mu = 10^{-3}$ Pa $\times$ s) is $D_T = k_B T/(6\pi\mu R) \approx 10^{-13}$ m^2/s and thus the translational Péclet number of the particle is $\mathrm{Pe_P} = V^{(b)}R/D_T \approx 50$. The rotational Péclet number of the particle, which we define as $\mathrm{Pe_R} := \Omega/D_R$, corresponding to the maximum magnitude of the angular velocity (attained at $\psi = \pi/2$, see (32)) is ((38), (29), (8), and $\mathbf{V}^{(b)}$ as given at the end of section 2.1)

$$\begin{aligned}\mathrm{Pe_R} &:= \frac{A^{(vp)}\Omega_0}{D_R} = \frac{1}{32}\left(\frac{R}{h}\right)^3 \frac{Q\Delta}{D}\frac{4}{3}\frac{R^2}{D_T} \\ &= \frac{1}{16}\frac{1}{|a_1^{(vp)}|}\left(\frac{R}{h}\right)^3 \frac{R\Delta}{|b|}\frac{V^{(b)}R}{D_T} = \frac{1}{4}\left(\frac{R}{h}\right)^3 \frac{R\Delta}{|b|}\mathrm{Pe_P}\,.\end{aligned} \tag{39}$$

This implies that for, e.g., $h = 2R$ one has $\mathrm{Pe_R} \approx 1.6\,(R\Delta/|b|)$. Therefore the rotation of $\mathbf{d}$ towards the direction of the surface-chemistry gradient, as induced by the response of the wall, dominates over the rotational diffusion (caused by the thermal fluctuations of the orientation of the particle) in regions with steep variations of the surface chemistry, i.e., for $\Delta \gg |b|/R$; e.g., the effect is very pronounced near sharp chemical steps as studied in [74]. This condition may be significantly relaxed if the particle is constrained to move at smaller distances h from the wall, which increases $\mathrm{Pe_R}$. However, in such cases

the validity of the point-particle analysis presented here must be carefully cross-checked against full numerical solutions. Finally, we note that if the surface-chemistry gradients fulfill $\Delta \approx |b|/R$), rotational diffusion and deterministic aligning are competing effects of similar magnitude. Therefore, in this case we expect the motion to exhibit noisy oscillations around a state which appears to be aligned on average.

4. Summary and conclusions

We have shown that a chemically active colloid, which moves in the vicinity of a chemically heterogeneous wall, can detect these variations in the chemical composition of the wall via induced osmotic flows which couple back to the colloid. For a constant surface-chemistry gradient along the wall, the colloid exhibits a tendency to align its axis with the direction of this gradient. This phenomenon, which is a primitive form of guidance by sensing the environment, resembles that of thigmotaxis, i.e., a response to the proximity of a physical change in the environment as exhibited by living organisms.

By employing a point particle approximation (section 2.2 and section 2.3) we have characterized this phenomenon by calculating the angular velocity of the rotation of the axis of the particle induced by the osmotic flows generated at the wall ((24) and (15)). This is determined in leading order ((32)), by the "dipole" coefficient a_1 ((3) and (4)), of the chemical activity. This coefficient also determines the motility of the colloid in an unbounded fluid, under the proviso that the phoretic mobility coefficient b (see (5)) is uniform over its surface (see section 2.1). This allows us to conclude that the emergence of thigmotaxis, i.e., $\Omega \neq 0$, is a generic feature for active colloids which are motile in an unbounded fluid, which requires $a_1 \neq 0$ (see above (8)).

By using several simple models of active colloids, in section 3.2 we have shown (see (38)) that the thigmotactic alignment depends only weakly on the precise details of the chemical activity and thus of the motility mechanism. Finally, we have estimated ((39)) the magnitude of the surface-chemistry gradients needed so that the tendency for thigmotaxis dominates over the thermal fluctuations of the orientation $\mathbf{d}$ of the colloid in a plane parallel to the wall.

Once $\mathbf{d}$ is aligned with the direction $\nabla_{||} b_w$ of the surface-chemistry gradient at the wall, the distribution of the solute number density at the wall (see figure 2) and the response of the wall (via the chemi-osmotic coefficient b_w ((11))) have mirror-symmetry with respect to the plane which includes $\mathbf{d}$ and is normal to the wall (see figure 2). This ensures that a wall-induced translation along the y-direction, i.e., perpendicular to the surface-chemistry gradient (see figure 1(b)), vanishes in this state, i.e., $V_y^{(w)} = 0$. The translation V_x along the direction of the surface-chemistry gradient depends on all the details of the wall chemistry, including, via $V_x^{(w)}$ (see $(21a)$), the local value $b_w(\boldsymbol{\rho}_0)$ of the osmotic mobility coefficient at the lateral position $\boldsymbol{\rho}_0$ of the colloid, as well as, via $V^{(sd)}$ (see section 2.2, first sub-problem), on the details of the motility mechanism of the particle. Therefore this aspect was not pursued here further.

Finally we note that the emergence of thigmotaxis, as studied here, raises the

question of whether this can provide an effective mechanism for "source detection" problems, e.g., if the surface-chemistry gradient of the wall is not constant but rather decays with the distance from a point or a line. This generalizes the case of step-like variations in b_w which were studied in Ref. [74].

Acknowledgments

M.N.P. and W.E.U. acknowledge financial support from the German Science Foundation (DFG), grant no. TA 959/1-1.

References

[1] Ismagilov R F, Schwartz A, Bowden N and Whitesides G M 2002 *Angew. Chem. Int. Ed.* **41** 652 – 654
[2] Paxton W F, Kistler K C, Olmeda C C, Sen A, St Angelo S K, Cao Y Y, Mallouk T E, Lammert P E and Crespi V H 2004 *J. Am. Chem. Soc.* **126** 13424 – 13431
[3] Ozin G A, Manners I, Fournier-Bidoz S and Arsenault A 2005 *Adv. Mater.* **17** 3011 – 3018
[4] Paxton W F, Sundararajan S, Mallouk T E and Sen A 2006 *Angew. Chem. Int. Ed.* **45** 5420 – 5429
[5] Solovev A A, Mei Y F, Urena E B, Huang G S and Schmidt O G 2009 *Small* **5** 1688 – 1692
[6] Mirkovic T, Zacharia N S, Scholes G D and Ozin G A 2010 *Small* **6** 159 – 167
[7] Howse J R, Jones R A L, Ryan A J, Gough T, Vafabakhsh R and Golestanian R 2007 *Phys. Rev. Lett.* **99** 048102:1–4
[8] Tung-Chun L, Alarcón-Correa M, Miksch C, Hahn K, Gibbs J G and Fischer P 2014 *Nano Letters* **14** 2407 – 2412
[9] Palacci J, Sacanna S, Steinberg A S, Pine D J and Chaikin P M 2013 *Science* **339** 936 – 940
[10] Baraban L, Tasinkevych M, Popescu M N, Sánchez S, Dietrich S and Schmidt O G 2012 *Soft Matter* **8** 48 – 52
[11] Gao W, Uygun A and Wang J 2012 *J. Am. Chem. Soc.* **134** 897 – 900
[12] Jiang H, Yoshinaga N and Sano M 2010 *Phys. Rev. Lett.* **105** 268302:1–4
[13] Qian B, Montiel D, Bregulla A, Cichos F and Yang H 2013 *Chem. Sci.* **4** 1420 – 1429
[14] Buttinoni I, Volpe G, Kümmel F, Volpe G and Bechinger C 2012 *J. Phys.: Condens. Mat.* **24** 284129:1–6
[15] ten Hagen B, Kümmel F, Wittkowski R, Takagi D, Löwen H and Bechinger C 2014 *Nature Comm.* **5** 4829:1–7
[16] Wang X, In M, Blanc C, Nobili M and Stocco A 2015 *Soft Matter* **11** 7376 – 7384
[17] Ebbens S J and Howse J R 2010 *Soft Matter* **6** 726 – 738
[18] Hong Y, Velegol D, Chaturvedi N and Sen A 2010 *Phys. Chem. Chem. Phys.* **12** 1423 – 1435
[19] Purcell E M 1977 *Am. J. Phys.* **45** 3 – 11
[20] Lauga E and Powers T R 2009 *Rep. Prog. Phys.* **72** 096601:1–36
[21] Spagnolie S and Lauga E 2010 *Phys. Fluids* **22** 081902:1–18
[22] Spagnolie S E and Lauga E 2012 *J. Fluid Mech.* **700** 105 – 147
[23] Pooley C M, Alexander G P and Yeomans J M 2007 *Phys. Rev. Lett.* **99** 228103:1–4
[24] Golestanian R, Yeomans J M and Uchida N 2011 *Soft Matter* **7** 3074 – 3082
[25] Zöttl A and Stark H 2012 *Phys. Rev. Lett.* **108** 218104:1–4
[26] Golestanian R, Liverpool T B and Ajdari A 2005 *Phys. Rev. Lett.* **94** 220801:1–4
[27] Ajdari A and Bocquet L 2006 *Phys. Rev. Lett.* **96** 186102:1–4
[28] Golestanian R, Liverpool T B and Ajdari A 2007 *New J. Phys.* **9** 126:1–9
[29] Jülicher F and Prost J 2009 *Eur. Phys. J. E* **29** 27 – 36

[30] Popescu M N, Dietrich S, Tasinkevych M and Ralston J 2010 *Eur. Phys. J. E* **31** 351 – 367
[31] Popescu M N, Tasinkevych M and Dietrich S 2011 *EPL* **95** 28004:1–6
[32] Golestanian R 2009 *Phys. Rev. Lett.* **102** 188305:1–4
[33] Ebbens S, Tu M, Howse J R and Golestanian R 2012 *Phys. Rev. E* **85** 020401(R):1–4
[34] Sabass B and Seifert U 2012 *J. Chem. Phys.* **136** 064508:1–15
[35] Sabass B and Seifert U 2012 *J. Chem. Phys.* **136** 214507:1–13
[36] Sharifi-Mood N, Koplik J and Maldarelli C 2013 *Phys. Fluids* **25** 012001:1–34
[37] Crowdy D G 2013 *J. Fluid Mech.* **735** 473 – 498
[38] Soto R and Golestanian R 2015 *Phys. Rev. E* **91** 052304:1–9
[39] Michelin S and Lauga E 2015 *Eur. Phys. J. E* **38** 7:1–16
[40] Uspal W E, Popescu M N, Dietrich S and Tasinkevych M 2015 *Soft Matter* **11** 434 – 438
[41] Masoud H and Stone H A 2014 *J. Fluid Mech.* **741** R4:1–7
[42] Bickel T, Majee A and Würger A 2013 *Phys. Rev. E* **88** 012301:1–6
[43] Würger A 2014 *J. Fluid Mech.* **752** 589 – 601
[44] Malgaretti P, Popescu M N and Dietrich S 2016 *Soft Matter* **12** 4007 – 4023
[45] Ruckner G and Kapral R 2007 *Phys. Rev. Lett.* **98** 150603:1–4
[46] Tao Y G and Kapral R 2008 *J. Chem. Phys.* **128** 164518:1–8
[47] Reigh S Y and Kapral R 2015 *Soft Matter* **11** 3149 – 3158
[48] de Graaf J, Rempfer G and Holm C 2015 *IEEE Trans. NanoBiosci.* **14** 272 – 288
[49] Wensink H H, Dunkel J, Heidenreich S, Drescher K, Goldstein R E, Löwen H and Yeomans J M 2012 *Proc. Nat. Acad. Sci.* **109** 14308–14313
[50] Marchetti M C, Joanny J F, Ramaswamy S, Liverpool T B, Prost J, Rao M and Simha R A 2013 *Rev. Mod. Phys.* **85** 1143 – 1189
[51] Elgeti J, Winkler R G and Gompper G 2015 *Rep. Prog. Phys.* **78** 056601:1–50
[52] Reinmüller A, Oğuz E C, Messina R, Löwen H, Schöpe H and Palberg T 2013 *Eur. Phys. J. ST* **222** 3011 – 3022
[53] Theurkoff I, Cottin-Bizonne C, Palacci J, Ybert C and Bocquet L 2012 *Phys. Rev. Lett.* **108** 268303:1–5
[54] Joanny J F, Jülicher F, Kruse K and Prost J 2007 *New J. Phys.* **9** 422:1–17
[55] Palacci J, Cottin-Bizonne C, Ybert C and Bocquet L 2010 *Phys. Rev. Lett.* **105** 088304:1–4
[56] Masoud H and Shelley M J 2014 *Phys. Rev. Lett.* **112** 128304:1–5
[57] Ginot F, Theurkauff I, Levis D, Ybert C, Bocquet L, Berthier L and Cottin-Bizonne C 2015 *Phys. Rev. X* **5** 011004:1–8
[58] Cates M E and Tailleur J 2015 *Ann. Rev. Condens. Matter Phys.* **6** 219 – 244
[59] Derjaguin B V, Yalamov Y I and Storozhilova A I 1966 *J. Colloid Interface Sci.* **22** 117 – 125
[60] Anderson J L 1989 *Ann. Rev. Fluid Mech.* **21** 61 – 99
[61] Das S, Garg A, Campbell A, Howse J, Sen A, Velegol D, Golestanian R and Ebbens S 2015 *Nat. Comm.* **6** 8999:1–10
[62] Simmchen J, Katuri J, Uspal W, Popescu M, Tasinkevych M and Sánchez S 2016 *Nat. Comm.* **7** 10598:1–9
[63] Mozaffari A, Sharifi-Mood N, Koplik J and Maldarelli C 2016 *Phys. Fluids* **28** 053107:1–35
[64] Hu J, Wysocki A, Winkler R G and Gompper G 2015 *Sci. Rep.* **5** 9586:1–7
[65] Uspal W E, Popescu M N, Dietrich S and Tasinkevych M 2015 *Soft Matter* **11** 6613 – 6632
[66] Campbell A I and Ebbens S J 2013 *Langmuir* **29** 14066 – 14073
[67] Enculescu M and Stark H 2011 *Phys. Rev. Lett.* **107** 058301:1–4
[68] Leshansky A M, Golovin A A and Nir A 1997 *Phys. Fluids* **9** 2818 – 2827
[69] Lauga A and Davis A 2012 *J. Fluid Mech.* **705** 120 – 133
[70] Domínguez A, Malgaretti P, Popescu M N and Dietrich S 2016 *Phys. Rev. Lett.* **116** 078301:1–5
[71] Palacci J, Sacanna S, Kim S H, Yi G R, Pine D J and Chaikin P M 2014 *Phil. Trans. R. Soc. A* **372** 20130372:1–19
[72] Palacci J, Sacanna S, Abramian A, Barral J, Hanson K, Grosberg A Y, Pine D J and Chaikin

P M 2015 *Science Advances* **1** e1400214:1–6
[73] Bregulla A P, Würger A, Günther K, Mertig M and Cichos F 2016 *Phys. Rev. Lett.* **116** 188303:1–5
[74] Uspal W E, Popescu M N, Dietrich S and Tasinkevych M 2016 *Phys. Rev. Lett.* **117** 048002:1–5
[75] Blake J R 1971 *J. Fluid Mech.* **46** 199 – 208
[76] Michelin S and Lauga E 2014 *J. Fluid Mech.* **747** 572 – 604
[77] Happel J and Brenner H 1983 *Low Reynolds number hydrodynamics* (Boston: Kluwer)
[78] Lorentz H A 1896 *Zittingsverslag van de Koninklijke Akademie van Wetenschappen te Amsterdam* **5** 168 – 175
[79] Kuiken H K 1996 *J. Eng. Math.* **30** 19 – 24
[80] Kim S and Karrila S J 1991 *Microhydrodynamics: Principles and Selected Applications* (Boston: Butterworth-Heinemann)
[81] Goldman A, Cox R and Brenner H 1967 *Chem. Eng. Sci.* **22** 637 – 651
[82] Brown A and Poon W 2014 *Soft Matter* **10** 4016 – 4027